

CONTROLLED OXYGEN LEVELS  
DURING KIDNEY MACHINE PERFUSION

By  
EWOUT BERGSMA

DRAFT GRADUATION REPORT

Submitted to  
Hanze University of Applied Science Groningen

in partial fulfillment of the requirements  
for the degree of

Fulltime Honours Bachelor Advanced Sensor Applications

2019



## ABSTRACT

### CONTROLLED OXYGEN LEVELS DURING KIDNEY MACHINE PERFUSION

By

EWOUT BERGSMA

The surgical research laboratory at the University Medical Center aims to improve their system that pumps blood (or substitute) through kidneys, while outside of the body, for research applications. Literature suggests that during this process high levels of oxygen in the blood should be avoided when pumping at normal temperatures (37 °C). Additionally the concept of adjusting for different needs of kidneys is explored as well. Therefore the goal of this project is to build a solution for an automated system that can dynamically control the oxygen level in a kidney perfusion machine for research applications. A conceptual model was created that made use of dynamically combining gases to the artificial lung in order to influence the oxygen level in the blood. Ultimately with the goal of keeping the oxygen levels in the blood coming out of the kidney at a constant. The latter with the hypothesis that a kidney that consumes less also requires less oxygen. The system was able to do this within a  $\pm 10\%$  margin during a stress test (n=1).

## DECLARATION

I hereby certify that this report constitutes my own product, that where the language of others is set forth, quotation marks so indicate, and that appropriate credit is given where I have used the language, ideas, expressions or writings of another.

I declare that the report describes original work that has not previously been presented for the award of any other degree of any institution.

Signed,

A handwritten signature in black ink, consisting of a large, stylized 'E' followed by a 'B' and a long horizontal stroke extending to the right.

EWOUT BERGSMA

## ACKNOWLEDGEMENTS

I would like to express my sincere gratitude to prof. dr. H.G.D. Henri Leuvenink for providing me the opportunity to do my graduation project. Without this opportunity and provided resources this project would have never been realized. Together with dr. Cyril Moers excellent advice was provided, for which I am grateful. Names which can not be mentioned without dr. Maarten Nijsten, whose sense of inclusion and ideas have supported me and the project.

I would like to extend my gratitude to Corina Vogt, for her comprehensive and professional support on behalf of the Hanze University of Applied Science Groningen. Additionally, I would like to show my appreciation for the technical assistance provided by dr. Felipe Nascimento Martins.

I must also thank all colleagues that have not only assisted professionally but also created an excellent atmosphere both in and outside the laboratory. Particularly helpful to me during this time were Jacco Zwaagstra, Petra Ottens, Kate Lewis, Leonie van Leeuwen, Rinse Ubbink, Tobias Huijink, Jaël Vos and Stan Hiemstra.

Impossible to forget is my special thanks to friends and family for their love and support.

## TABLE OF CONTENTS

List of Tables . . . . .	8
List of Figures . . . . .	9
<b>1 Rationale</b>	<b>10</b>
1.1 Research question . . . . .	11
<b>2 Situational &amp; theoretical analysis</b>	<b>12</b>
2.1 Slaughterhouse model . . . . .	12
2.2 Perfusion machine . . . . .	13
2.3 Oxygen dissociation curve . . . . .	13
2.4 Cellular respiration . . . . .	15
2.5 Oxygenator . . . . .	15
2.6 Rotameter . . . . .	15
2.7 Perfusion solution . . . . .	16
2.8 Requirements . . . . .	16
2.9 Oxygen sensors . . . . .	17
2.9.1 Gaseous oxygen . . . . .	17
2.9.2 Oximetry . . . . .	18
2.9.3 Dissolved oxygen . . . . .	18
2.10 Control . . . . .	20
2.11 Gas flow sensors . . . . .	20
<b>3 Conceptual model</b>	<b>21</b>
3.1 Oxygen sensor . . . . .	21
3.2 Control . . . . .	22
3.3 Gas flow sensor . . . . .	22
3.4 Feedback loop design . . . . .	22
<b>4 Research design</b>	<b>24</b>
4.1 Response time of the oxygen sensor . . . . .	24
4.1.1 Effect of flow rate . . . . .	24
4.1.2 Response time to different deltas . . . . .	24
4.2 Desired steady state of the gas mixture . . . . .	25
4.3 Gas flow subsystem . . . . .	26
4.3.1 Sensor calibration . . . . .	26
4.3.2 PID tuning . . . . .	26
4.4 Oxygen PID tuning . . . . .	26
4.5 Validation . . . . .	27
<b>5 Results</b>	<b>28</b>
5.1 Response time of the oxygen sensor . . . . .	28
5.1.1 Effect of flow rate . . . . .	28
5.1.2 Response time to different deltas . . . . .	29
5.2 Desired steady state of the gas mixture . . . . .	30
5.3 Gas flow subsystem . . . . .	31
5.3.1 Sensor calibration . . . . .	31
5.3.2 PID tuning . . . . .	33
5.4 Oxygen PID tuning . . . . .	34
5.5 Validation . . . . .	36

<b>6</b>	<b>Conclusion</b>	<b>38</b>
<b>7</b>	<b>Discussion</b>	<b>38</b>
<b>8</b>	<b>List of definitions</b>	<b>39</b>
<b>9</b>	<b>References</b>	<b>40</b>
<b>10</b>	<b>Appendix</b>	<b>43</b>
A	Sniffing the random access memory for data acquisition . . . . .	43
B	To be added . . . . .	44

## LIST OF TABLES

1	List of gas densities at standard conditions for temperature and pressure [15]. Carbogen defined as a mixture of 95% oxygen and 5% nitrogen. . . . .	16
2	List of potential online dissolved optical oxygen sensors. Range and accuracy converted to hPa at 37°C and 1160 hPa pressure, physiological values [21]. Ocean Optics products require a custom part to enable online capability, excluded from price. Response time defined as 90% of a signal measured during a transition from an air saturated to an oxygen deprived solution [36, 37]. . . . .	19
3	List of potential proportional valves. Shipping prices in brackets. . . . .	20
4	List of potential gas flow sensors. . . . .	20
5	Table with results of the effect of flow rate on the response time of the dissolved oxygen sensor. First group experienced a flow rate of 150 ml/min, the second group 575 ml/min. . . . .	28
6	Table with results of the response times to different changes in oxygen level. The group with a 610 $\Delta$ hPa was added to investigate statistical difference. . . . .	29
7	Table with the results of the experiment that researched the ratio between nitrogen and carbogen supplied to the oxygenator in order to find a 133 hPa dissolved oxygen level. . . . .	30
8	Calibration results for the gas flow sensor. . . . .	31
9	Table of proportional, integral and derivative gain for the gas flow subsystem. . . .	33
10	Table of gains from two different kidneys subjected to identical step inputs. . . . .	35



## LIST OF FIGURES

1	Image of the cannula used during the project. The left side connects to the perfusion machine, the right side inserts into the artery. . . . .	12
2	Kidney prepared at slaughterhouse. . . . .	12
3	Schematic representation of the current perfusion machine. Carbogen is a gas mixture consisting of 95% oxygen and 5% carbon dioxide. The oxygenated perfusion solution depicted in red, perfusion solution with lower oxygen levels depicted in blue. . . . .	13
4	ODC in a theoretical healthy human [16]. Vertical axis: Hemoglobin (Hb) saturation, horizontal axis: $PO_2$ , partial pressure of oxygen. . . . .	14
5	Image of a Medos Hilite 1000. . . . .	16
6	Image of a Louchen rotameter. . . . .	16
7	Optical oxygen sensor principle [33]. . . . .	19
8	Schematic representation of the conceptual model. . . . .	21
9	Diagram of the PID control, the gas flow PID (green) nested inside of the oxygen PID (orange). . . . .	23
10	Schematic representation of the response time experiment setup. . . . .	24
11	Schematic representation of the desired steady state setup. . . . .	25
12	Diagram of the PID control which will be tuned in this experiment. Diagram identical to the inner (green) loop seen in figure 9. . . . .	26
13	Diagram of the PID control. The outer loop has been tuned in this experiment. Diagram identical to the loop seen in figure 9, excluding the colors. . . . .	27
14	Histogram of the results of the effect of flow rate on the response time of the dissolved oxygen sensor. First group experienced a flow rate of 150 ml/min, the second group 575 ml/min. A statistical significant difference between the two groups was observed. . . . .	28
15	Graph. . . . .	29
16	Graph of the ratio between nitrogen and carbogen in order to achieve an oxygen level of 133 hPa, alongside a linear fit. . . . .	30
17	Graph. . . . .	31
18	Plots of the input and resulting output of the gas flow subsystem during a series of step inputs. . . . .	33
19	Plots of the response of the mathematical model and the actual response given the same input, for the gas flow subsystem. . . . .	33
20	Plots of the input and resulting output of the full system during a series of step inputs. Input in carbogen flow (ml/min) depicted in green, output in venous oxygen level (hPa) depicted in blue. . . . .	34
21	Plots of the response of the mathematical model and the actual response given the same input, for the full system. Mathematical model depicted in red, actual model in blue. . . . .	34
22	Second set of plots of the response of the mathematical model and the actual response given the same input, for the full system. Mathematical model depicted in red, actual model in blue. Kidney endured multiple ischemic periods and data of the last step impulse was lost due to technical difficulties. . . . .	35
23	Graph with temperature data of the validation experiment. . . . .	36
24	Graph with carbogen flow data of the validation experiment. . . . .	36
25	Graph with arterial oxygen pressure data of the validation experiment. . . . .	36
26	Graph with venous oxygen pressure data of the validation experiment. . . . .	37
27	Photo of the entire setup during the validation experiment. . . . .	37
28	Photo of the kidney during the validation experiment. . . . .	37

# 1 Rationale

New year's eve 2017, the Netherlands. According to the Dutch Transplantation Foundation, there are 1,115 patients waiting for organ donation, 673 of which are waiting for a kidney. 83% of the patients waiting for a kidney have to wait for at least a year and 15% have to wait five years or longer. There is a dramatic shortage. This shortage has led to extending the donor criterias, such as an increased use of donors of older age and donors that have experienced a loss of blood flow. Unfortunately, this does not come without consequences, as these donor organs are more susceptible to ischemia-reperfusion injury (IRI). IRI is damage caused by a lack of oxygenation, either caused by a lack of blood flow or an insufficient amount of oxygen before (artificially) restoring the blood and oxygen supply. This has negative results on the health and survival of the organ. This has led to a growing interest in research aimed at oxygenation during machine perfusion (MP) [1, 2]. MP is a technique that revolves around artificially supplying the organ with oxygenated blood or blood substitute, in order to supply the organ with oxygen in an attempt to reduce IRI. Ultimately with the goal of keeping the organ as healthy as possible during the transplantation process, including the transportation of the organ from the donor to the recipient.

Traditionally organ preservation was done by cooling and submerging the organ in a cold preservation solution and transporting it on melting ice, a method called cold storage (CS) [3]. Since then a method involving cold MP (4°C), called hypothermic machine perfusion (HMP), has been established in clinical practice [4]. This shift in technique adds three years to the survival of the kidney after transplantation due to the added oxygenation [5]. However, research suggests that MP during normal temperatures (37°C), a method called normothermic machine perfusion (NMP), may enhance the condition of the kidney when comparing it to the currently used HMP technique [6–8]. However, one of the current challenges during NMP is the excessive supply of oxygen. Currently, oxygenation during NMP typically happens at levels higher than normally found in nature. New insights suggest that non-excessive oxygen delivery might be of utmost benefit during NMP [9, 10]. Additionally, it appears to be the case that there is no default oxygen supply requirement by organs. Instead it should be tailored for the specific needs of the individual organ, which may change over time [9].

Therefore the goal of this project is to create an automated system that can dynamically control the oxygen level in the blood or blood substitute. Preferably one that can adjust for the specific need of the organ.

Although the clear and important clinical relevance of oxygenation during MP, this project will aim towards the research field. Naturally, as this is where innovation is supposed to start, but also as MP has its purpose in the research field. It allows an organ to be examined in an isolated environment, as it excludes other organs, opening the doors for a whole new type of research. A type in which the excluded organs do not influence the results of the organ of interest. Furthermore it can solve ethical problems, as organs that have been discarded for transplantation may be used, reducing the need of living subjects. A solution which may also help to reduce the amount of tests on animals, as some research may be shifted away from animal testing to MP research. Noteworthy not only for its ethical reasons, but also noteworthy as reduction of animal testing has been a subject the Dutch government has been pushing [11].

Important to note is that the project will focus on kidney MP. Mainly due to the fact that this is the specialization of the environment this project has taken place in, but also because excluding other organs helps with the feasibility of the project's time scope. Additionally, this document will use the term perfusion solution, as a term to include both blood and blood substitutes in the MP context.

## 1.1 Research question

“How can one build a solution for an automated system that can dynamically control the oxygen level in a kidney perfusion machine for research applications?”

- What type of oxygen sensor is the best fit for the system?
- How should the oxygen level be influenced by the system?
- How can the system adjust for the different oxygen requirements of the kidney?
- How well does the conceptual model perform?

## 2 Situational & theoretical analysis

### 2.1 Slaughterhouse model

The surgical research laboratory of the University Medical Center, the area this project has taken place in, has a model that supplies them with the kidneys required for their research. This subsection is dedicated to explaining the procedure the laboratory follows, in order to get a better understanding of the current situation. The source of information originates from proprietary documentation and verbal communication with the laboratory managers.

The laboratory uses porcine organs for most of their research, due to being similar to human organs [12]. Porcine kidneys are obtained from a nearby slaughterhouse. The employees there have been carefully instructed on how to retrieve the kidneys, such that they are not damaged and remain suitable for research. Once the kidneys are retrieved they are handed over to the researcher, including the corresponding blood would the researcher have requested this. Whether the researcher requires blood depends on their specific research. The researcher will then prepare the kidney, by removing excessive fat and preparing the artery such that it can be cannulated. A cannula, as seen in figure 1, is a special piece of tubing which will be partially inserted into the aorta such that the kidney can be attached to the perfusion machine later. Afterwards the kidney will be flushed with a cold solution using a syringe, such that the remaining blood is removed but also to start the cooling of the kidney.

The CS and HMP preservation methods mentioned in the rationale are the two available options for transportation. Both of these methods happen at low temperatures in order to lower the metabolic rate, in order to enhance the preservation. HMP has an advantage in terms of preservation over CS, but practically CS is a simpler method as it excludes all of the extra hardware required by the added oxygenation which the HMP method provides [13].

Once the kidney arrives at the laboratory the kidney is taken out of CS or HMP and is attached to the perfusion machine, assuming the intend of the research is to perform NMP.



*Figure 1: Image of the cannula used during the project. The left side connects to the perfusion machine, the right side inserts into the artery.*



*Figure 2: Kidney prepared at slaughterhouse.*

## 2.2 Perfusion machine

The concept of the current existing perfusion machine, of which the product of this project has to collaborate is displayed in figure 3:

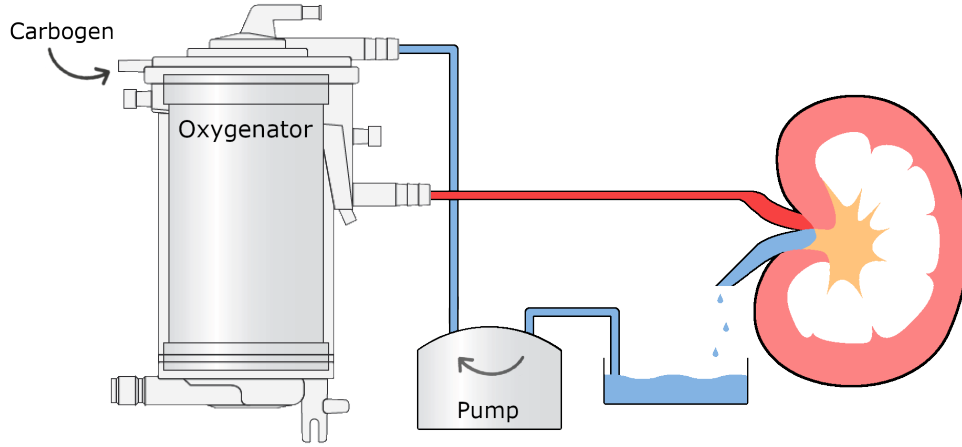


Figure 3: Schematic representation of the current perfusion machine. Carbogen is a gas mixture consisting of 95% oxygen and 5% carbon dioxide. The oxygenated perfusion solution depicted in red, perfusion solution with lower oxygen levels depicted in blue.

The above figure merely shows the system without any sensors that might be added by the user. In this typical setup the oxygenator is supplied with carbogen, a gas consisting of 95% oxygen and 5% carbon dioxide. This gas is used by the oxygenator to oxygenate and to extract the carbon dioxide from the perfusion solution. Inside the oxygenator a membrane allows gas to move between the supplied gaseous mixture and the perfusion solution [14]. Which results in oxygenation of the perfusion solution and potentially extracting carbon dioxide produced by the kidney from said solution. The oxygenated perfusion solution then travels into the artery of the kidney, such that the kidney is supplied with oxygen. The perfusion solution then flows through the kidney, for it to eventually leave the kidney through the venous. From the venous the perfusion solution leaks into a bath which then ultimately gets pumped into the oxygenator, completing the full loop of the perfusion solution.

## 2.3 Oxygen dissociation curve

In order to gain a better understanding of the underlying principles that are associated with oxygenation this subsection will cover the forms of oxygen and their relationships that will be encountered. This understanding will become essential during the decision making of the type of oxygen sensor later in this document, but is also important for the entirety of this project. For the scope of this project oxygen can come in three different forms:

- Gaseous oxygen
- Dissolved in the perfusion solution
- Bound to an oxygen carrier

As can be seen in figure 3, oxygen enters the oxygenator in a gaseous form. Inside the oxygenator it dissolves into the perfusion solution. A process explained by Henry's law, which states that the amount of dissolved gas in a solvent is proportional to the partial pressure of the gas in contact with the solvent. E.g. given a beaker with water without a lid, the amount of dissolved oxygen in water is directly proportional to the partial pressure of the oxygen in air. This law is expressed as follows:

$$C = k * P_{gas}$$

In which C stands for the dissolved concentration, k for Henry's law constant and P for the partial pressure of the gas [15]. However in MP it is not only the dissolved oxygen that is important. Perfusion solutions can hold oxygen carriers, such as hemoglobin. These carriers can bind oxygen, extracting the oxygen from the solvent. During oxygen uptake this creates a situation in which oxygen dissolves into the solvent, after which it binds to the oxygen carrier. Consequently allowing new gaseous oxygen molecules to dissolve into the solvent. A reverse of this principle holds true during oxygen delivery [16].

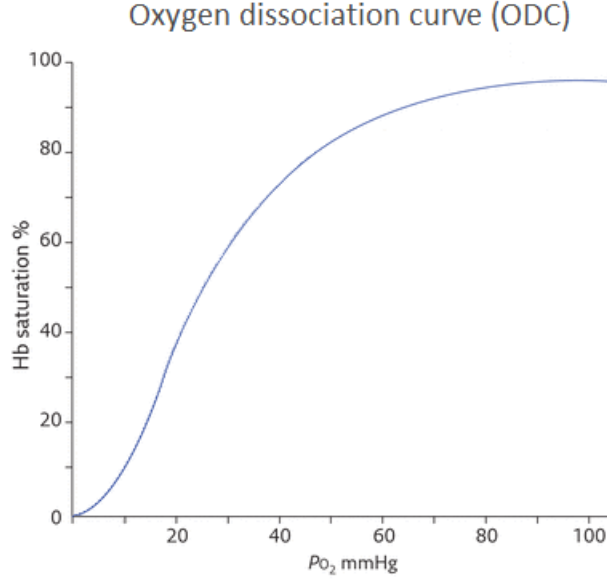
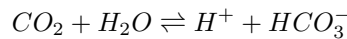


Figure 4: ODC in a theoretical healthy human [16]. Vertical axis: Hemoglobin (Hb) saturation, horizontal axis: PO<sub>2</sub>, partial pressure of oxygen.

Figure 4 shows a graphical representation of the relationship between the hemoglobin saturation and the partial pressure of oxygen, a relation with the name oxygen dissociation curve (ODC). The affinity of an individual hemoglobin molecule for oxygen increases as the amount of oxygen bound to the hemoglobin increases. This explains the initial increase in slope. Consequently the chances of oxygen molecules binding decreases as the hemoglobin saturation increases, completing the sigmoid shape of the curve. Additionally there are multiple factors that decrease the overall slope of the curve, opposites (e.g. increasing instead of decreasing a factor) increases the slope of the overall curve [16, 17]:

- Decrease in pH
- Increase in temperature
- Increase in partial pressure of carbon dioxide

The influence of carbon dioxide factor on the ODC is explained by a phenomenon called the Bohr effect [18]. This effect is partially explained by the following underlying biochemical reaction:



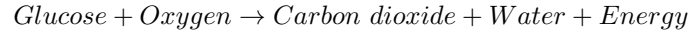
As can be seen in the formula, an increase of carbon dioxide (CO<sub>2</sub>) results in an increase of H<sup>+</sup> and thus decreases the pH. The change in pH influences the slope of the ODC, as mentioned above [19]. However, the change in pH is not the only way carbon dioxide influences the slope of the ODC. The partial pressure of carbon dioxide itself increases the slope of the ODC, independent of the change in pH [16, 20]. Although, the independent influence of carbon dioxide on the ODC appears to be small. As under conditions normally found in humans (37°C, 7.3 pH and 118.7 hPa oxygen) an

artificial carbon dioxide change of 53.3 hPa to 106.7 hPa influences the hemoglobin saturation by less than 1% [17].

Additionally, important to note is that a change in concentration of hemoglobin is proportional to the total oxygen delivery of the perfusion solution. Logically, as less oxygen carriers translate into less oxygen transportation.

## 2.4 Cellular respiration

For metabolism in mammals and for the scope of this project cellular respiration plays a key factor. Cellular respiration is a process in which larger molecules are broken down into smaller molecules, ultimately netting energy. The combination of steps can be summarized as follows [21]:



In isolation this information would suggest that monitoring the amount of one of the components would allow to comprehend all of the formula. E.g. knowing the amount of oxygen consumed in a kidney gives direct insight on the amount of energy that has been extracted. However, this is not the case. The oxygen to carbon dioxide relation can be expressed using the respiratory quotient (RQ) which describes the volumetric ratio between the total consumed oxygen and the carbon dioxide evolved from oxygen in an organism. By monitoring it can be observed that RQs ranging from less than 0.7 to up to 0.8 can be found in humans [22]. Therefore expressing the flaws in just monitoring oxygen when requiring information regarding the cellular respiration.

A possible oxygen consuming process is the creation of reactive oxygen species, which in excessive amounts results in oxidative stress. This stress results into cell and kidney damage [23]. At oxygen levels higher than normally found in nature called supraphysiological oxygen levels, mitochondria respond with creating a burst of ROS [24, 25]. Therefore demonstrating the importance of monitoring oxygen levels and avoiding supraphysiological oxygen levels.

## 2.5 Oxygenator

An UMCG specific study regarding an alternative to the currently used oxygenator has not led to a different oxygenator for kidney MP research at the UMCG [26]. Additionally, a system is in place that enables oxygenators to be reused for research purposes. These oxygenators have been previously used in the clinic. For these reasons and as a manner to keep the financial stress at a minimum the Medos Hilite 1000 will be considered exclusively. Figure 5 shows an image of the Medos Hilite 1000.

Relevant specifications of the Medos Hilite 1000 [14]:

- Maximum gas flow rate: 2.0 l/min
- Blood flow rate range: 0.15 - 1.0 l/min

## 2.6 Rotameter

As has become apparent, this project will involve gases. Typically, the laboratory uses rotameters for volumetric flow rate measurements. Parts of the research design of this project will make use of these available rotameters. A rotameter consists of a tube with a float inside, as can be seen in figure 6. In this figure the float has the shape of a sphere, however different types of floats are available. The gas of which the flow rate is to be measured travels through the tube. The drag created by the travelling gas pushes the float upwards, while gravity pulls the float downwards, assuming the rotameter is in an upright position such that gravity pulls in parallel direction to the rotameter. This relation allows to measure the flow rate of the gas travelling through the tube [27].

Rotameters are typically calibrated for a medium with a set density, thus being incorrect for all mediums with different densities [27, 28]. However, for conversion between one gaseous medium to another the following formula can be used [28]:

$$K = \sqrt{\frac{D_{calibrated}}{D_{measured}}}$$

Where K is the conversion factor,  $D_{calibrated}$  and  $D_{measured}$  are the densities of the original calibrated gas and the actual measured gas. See table 1 for a list of gas densities:

	$O_2$	$N_2$	$N_2O$	$CO_2$	Carbogen
Density (g/L)	1.429	1.251	1.834	1.977	1.456

Table 1: List of gas densities at standard conditions for temperature and pressure [15]. Carbogen defined as a mixture of 95% oxygen and 5% nitrogen.



Figure 5: Image of a Medos Hilite 1000.



Figure 6: Image of a Louchen rotameter.

## 2.7 Perfusion solution

Perfusion solutions used in MP can be divided into two groups. One group with and the other without oxygen carriers. As previously discussed, literature appears to agree on the necessity of avoiding non-physiological oxygen levels during NMP. Furthermore, during near-physiological thermal conditions oxygen carriers are important to meet the oxygen demand of the kidney [29]. In order to enable the system to meet the oxygen demand of the kidney during NMP the use of oxygen carriers appears to be unavoidable.

As explained the current slaughterhouse model, which the surgical research laboratory operates on, enables the supply of porcine organs. This includes the corresponding blood. Due to this model the laboratory has a time and cost effective supply of organs for research purposes. For this reason and due to the significantly higher cost of perfusion solutions with oxygen carriers this project will exclusively use blood when deemed necessary. This however does not mean that other types of perfusion solutions should be neglected during considerations of design choices.

## 2.8 Requirements

One of the main challenges is to set the initial requirements of the system. The unprecedented intents of this project disallow comparing or getting inspiration from an existing system. Moreover, to an extend it is unknown what the requirements of an ideal solution are, without extensive research. Possibly the outcome of this project may contribute to such research. Before then the best efforts within the scope of this project are to make educated estimations. Whenever necessary small-scale



experiments will be conducted.

The answer to finding the range in which the oxygen sensor has to perform might come from physiology. However using physiological values in a MP context requires upmost care. In the context of this project the only organ within the system is the kidney. Logically, as excluding all other organs means that all of their functions are lost simultaneously. Therefore MP conditions will deviate from physiology. Though research suggests that during NMP supraphysiological oxygen levels should be avoided, as mentioned previously [9, 10]. Therefore the best estimation to the range in which the oxygen sensor has to perform is to at least cover the physiological range, which is from 45 hPa to 133,3 hPa [30].

A complex requirement to determine is the maximum expected change in oxygen level. The sensor should be able to measure correct values even if there is a sudden change in oxygen level. However no data in literature was found regarding the partial pressure of oxygen during extreme changes in oxygen level. Nor can we extract valuable information from physiology, as MP researchers expose kidneys to changing conditions not found in physiology. E.g. when transferring a kidney from cold storage to NMP, increasing the metabolic rate and thus increasing oxygen consumption [9]. However from all the data regarding oxygen levels created by the surgical research laboratory of the University Medical Center Groningen (UMCG) one experiment emerges. The yet unpublished work by Hanno Maassen researches the possibilities regarding a hydrogen sulphide induced hypometabolic state. During this research a substantial sudden decrease in metabolic rate was observed through the use of hydrogen sulphide. From this data a maximum change of 325.8 hPa/min has been observed. For the scope of this project this observed change will be considered the maximum change of oxygen partial pressure that the sensor has to be able to measure.

In order to influence the oxygen levels in the perfusate one could attempt to achieve this by changing the carbogen flow. However this also influences the rate at which carbon dioxide can leave the oxygenator. E.g. during a situation in which the kidney suddenly requires lower amounts of oxygen restricting the carbogen flow may answer the change in oxygen demand, but will restrict the amount of carbon dioxide that can leave the perfusate. An increase in carbon dioxide results in a shifting ODC. In order to avoid this behaviour, rather than restricting the carbogen flow this project will investigate the viability of controlling the carbogen concentration. This will be done by adding nitrogen to a dynamic amount of carbogen supplied to the inlet of the oxygenator. More on the desired carbogen-nitrogen ratios will come forward in the research design.

Additional quantification of the requirements will become apparent in the remainder of this section and the results section.

## **2.9 Oxygen sensors**

As seen in figure 3, oxygen is present in both gaseous and dissolved form. The gaseous form is present at the gas inlet and potentially at the gas outlet of the oxygenator, the dissolved form is present in the perfusate. Both forms could be a potential solution to monitoring the oxygen level.

### **2.9.1 Gaseous oxygen**

Theoretically it is possible to monitor the oxygen level in the perfusate by sensing the gaseous oxygen levels. Knowing the amount of oxygen supplied into the gas inlet of the oxygenator and the amount of gaseous oxygen that exits the oxygenator gives insight on the total oxygen consumption. However multiple considerations have to be evaluated when choosing for this approach.

Firstly, by examining the commercially available gaseous oxygen sensors can be concluded that typical oxygen sensors sense the concentration of oxygen. In order to gain information regarding the oxygen content the sensor has to closely collaborate with a gas flow sensor. Potentially both at the

inlet and outlet, as gas both dissolves and condenses inside the oxygenator.

Secondly, adding sensors to the outlet of the oxygenator could add to the resistance the gas experiences. As a consequence the total pressure of the gas has to increase in order to keep the gas flow identical. Hypothetically this could have negative results on the membrane that divides the gas and the perfusate inside the oxygenator. These consequences could include reduced lifespan of the oxygenator and accumulation of gas in the perfusate. The latter due to a mismatch of pressures from both sides of the membrane, resulting in an excess of gas moving through it.

Thirdly, changes in the ODC results in a difference of oxygen entering and leaving the perfusate. Therefore changes in ODC will change the difference between in and out going gaseous oxygen content, thus influencing the measured values on top of influencing the oxygen consumption [21].

Lastly, it is not necessarily the case that all of the oxygen in the perfusate is directly consumed by the kidney. This means that some oxygen remains in the perfusate. Therefore, the system has no insight on the potential accumulation of oxygen that remains in the perfusate by exclusively monitoring the gaseous oxygen.

### **2.9.2 Oximetry**

Oximeters are used to measure the ratio of hemoglobin bound to oxygen molecules to the total amount of hemoglobin or an approximation thereof. Which results in a measurement of oxyhemoglobin saturation. The core principle on which oximeters and pulse oximeters operate are identical. Typically, two different lights each at a different wavelength are emitted in series. Each of the wavelengths are absorbed differently, one by hemoglobin bound to oxygen and the other by hemoglobin not bound to oxygen [16, 31, 32]. Important to note is that oximetry ignores dissolved oxygen and only performs a measurement on oxygen bound to hemoglobin.

One of the limitations during the use of oximetry is its response to anemia, a clinically used term for the deficiency of hemoglobin [32]. Informing that measurements done during oximetry are influenced by the hemoglobin concentration.

### **2.9.3 Dissolved oxygen**

Dissolved oxygen sensors can be divided into two groups, namely amperometric and optical. However the amperometric sensors consume oxygen, require more maintenance and calibration [33, 34]. All of which are undesirable for this project, therefore the remainder of this subsection will exclusively consider optical dissolved oxygen sensors.

Optical dissolved oxygen sensors operate on the principle of emission of light by a substance caused by previously absorbed light, called fluorescence. This substance, the luminophore, is located at the end of the sensor and is in contact with the liquid. The sensor emits a light after which the luminophore responds with emitting a light at a different wavelength. The lifespan of the light emitted by the luminophore is influenced by the presence of oxygen. Therefore, by measuring the lifespan a conclusion can be made regarding the concentration of oxygen [33]. A visual representation can be found in figure 7:

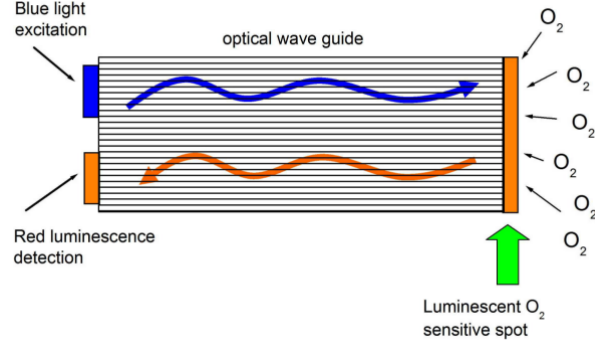


Figure 7: Optical oxygen sensor principle [33].

In order to monitor the oxygen consumption two dissolved oxygen sensors would have to be implemented. One at the artery and the other at the venous. However careful implementation of the sensor at the venous is necessary. Any type of contact between air and perfusate influences the oxygen level in the perfusate through Henry's law and any contact between air and sensor will influence measurement as the sensor can not sense the dissolved oxygen in the perfusate without being in contact with the perfusate.

Additionally it is important to note that dissolved oxygen sensors do not sense oxygen bound to an oxygen carrier, but exclusively measure the dissolved oxygen. Therefore, in order to supply a constant oxygen content while controlling on partial pressure the ODC should not shift. This requires a constant pH, temperature and concentration of hemoglobin. Which, judging by the research protocols of MP researches, is typically already a goal for prolonged periods during the MP researches for pH and temperature. The excluded constant hemoglobin concentration can be disturbed by subsequently added chemicals, however if deemed necessary then combining these chemicals with hemoglobin could keep the concentration constant. Furthermore, changes in these factors could theoretically be compensated for mathematically, but this will remain outside of the scope for this project [17]. In table 2 a selection of potential online dissolved oxygen sensors can be found:

Producer	Products	Range (hPa)	Accuracy (hPa)	Response time (s)	Cost (€ ex. VAT)
Ocean Optics [35]	NEOFOX-KIT-PROBE	0-230	$\pm 0.55$ at 11.5 $\pm 5.49$ at 229.9	Unknown	3,660
PreSens [36]	EOM-O2-FOM, FTC-PSt3	0-1330	$\pm 0.55$ at 2.19 $\pm 4.39$ at 229.29	<40	3,125
Pyro Science [37]	FSO2-1, TOFTC2	0-680	$\pm 0.30$ at 11.0 $\pm 3.0$ at 164.6	<9	3,580

Table 2: List of potential online dissolved optical oxygen sensors. Range and accuracy converted to hPa at 37°C and 1160 hPa pressure, physiological values [21]. Ocean Optics products require a custom part to enable online capability, excluded from price. Response time defined as 90% of a signal measured during a transition from an air saturated to an oxygen deprived solution [36, 37].

## 2.10 Control

In order to control the carbogen flow the system requires a proportional flow. A selection of low flow proportional valves can be found in table 3. Variable carbogen pressure of 0-4 bar differential pressure can be achieved at the surgical research lab. The incoming pressure of the gas from the perspective of the valve influences the maximum achievable flow.

Producer	Product	Flow rate (l/min)	Differential pressure (bar)	Hysteresis (%)	Cost (€ ex. VAT)
Aircom [38]	PVK-092	3	3.5	<10	109
Aircom [39]	PV202-004	5	10	<5	110
Baccara [40]	GEM-PR	1.1	12	Unknown	120 (+28.7)
Bürkert [41]	274910	1.2 per bar	10	5	185
Parker [42]	P910000200003	4.2 (2)	0.69 (0.18)	7	108.34 (+10)

Table 3: List of potential proportional valves. Shipping prices in brackets.

## 2.11 Gas flow sensors

From the datasheets of the proportional valves mentioned in table 3 can be understood that the relationship between control and flow is not linear [38–42]. Additionally, this relationship is influenced by the pressure at the intake and the hysteresis of the valve. A gas flow sensor could counteract these challenges by creating a feedback loop. Furthermore, with information regarding the gas flow the representation of the results become more meaningful, as a non-linear “control” axis can be replaced with a linear flow axis. Lastly the gas flow sensor could be used to signal the end user for any malfunctioning that might appear during typical usage, e.g. a gas leakage before the flow sensor preventing the system to reach the desired gas flow. A selection of gas flow sensors can be found in table 4:

Producer	Product	Flow rate (l/min)	Accuracy (%)	Cost (€ ex. VAT)
Honeywell [43]	AWM3300V	0-1	$\pm 1$	114
Omron [44]	D6F-P0010A1	0-1	$\pm 5$	60
Omron [45]	D6F-01A1-110	0-1	$\pm 3$	109
Omron [45]	D6F-02A1-110	0-2	$\pm 3$	115

Table 4: List of potential gas flow sensors.

### 3 Conceptual model

A diagram of the conceptual model can be found in figure 8. Rather than just carbogen entering the gas inlet of the oxygenator a dynamic mixture of carbogen and nitrogen will be supplied. Nitrogen will be kept at a constant flow, as the system is interested in achieving a range that is at the bottom of the full possible range of oxygen in the perfusate. By dynamically controlling the carbogen and thus the oxygen supply the system should be able reach the entire desired range. Details of this exact application will follow the results following section ??.

Adding two oxygen sensors, one at the arterial side and the other at the venous, will allow the monitoring of oxygen consumption, either implicitly with a constant ODC in mind or potentially by using mathematical models [17]. Directly using the data from at least one of the two sensors will allow for creating a control system with a feedback loop. By correctly tuning the processing unit a constant or dynamically controlled partial pressure of oxygen can be achieved, either at the artery or venous.

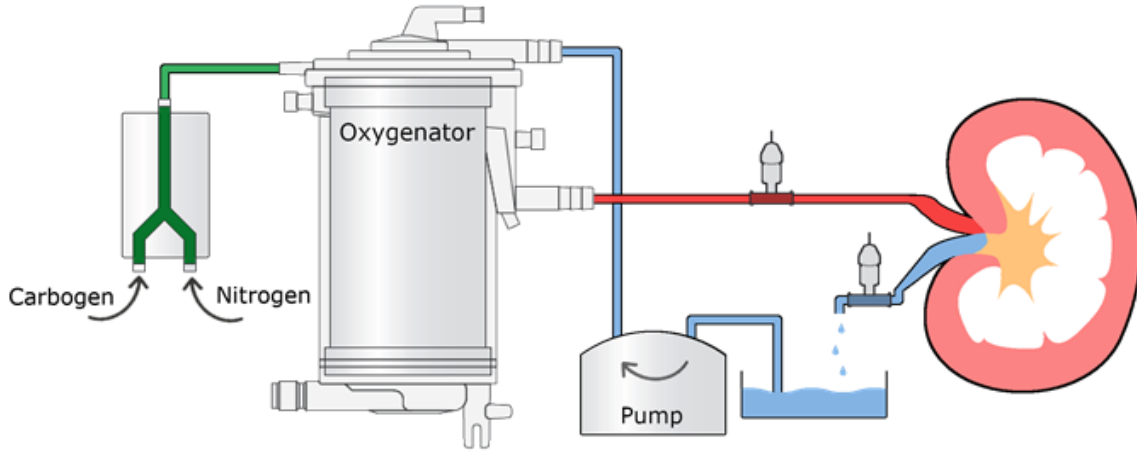


Figure 8: Schematic representation of the conceptual model.

#### 3.1 Oxygen sensor

Although gaseous oxygen sensors appear to be a theoretical viable option the practicality presents multiple challenges, as discussed before. Due to time constraints combined with the practical challenges and due to the fact that another group of engineers and researchers is currently researching this option a decision against gaseous oxygen sensors has been made for the scope of this project. Additionally a decision against oximetry has been made. Choosing for oximetry would disable any option to use the system without hemoglobin, e.g. during hypothermic machine perfusion (HMP) or when using perfusates with a different oxygen carrier. Furthermore, this avoids anemic based misreadings, giving the user liberty over the hemoglobin concentration.

This leaves dissolved oxygen sensors as the last option. However, as previously mentioned choosing for dissolved oxygen sensing requires to keep the ODC or any other relationship between partial pressure and oxygen carrier in mind. However, keeping the temperature, pH and hemoglobin constant appears to be feasible. From the list of potential sensors, found in table 2, the sensor made by Pyro Science appears to beat the competition. It has a better accuracy than both of its competitors and the response time is more than four times faster than the PreSens sensor. Nevertheless, this project will be using the PreSens sensor option, considering the substantial prices and the availability of the PreSens sensor at the laboratory. Unfortunately this presents a challenge in obtaining the data in order to be used in real-time, more on this in appendix A.

### 3.2 Control

Deciding which low flow proportional valve to choose from the selection found in table 3 brings a challenge. It is known that the oxygenator has a 2.0 l/min limit, but it is unknown how much of the total supply should be nitrogen or carbogen. Therefore an experiment will have to be set up. The results following this experiment inform a maximum desired carbogen flow of 0.5 l/min (see section 4.2). Furthermore, if possible a low incoming pressure to the valve could improve the user experience. Simply as lower pressures could prevent the tubing installed by the user to come loose.

From the list of potential proportional valves we can observe that the documentation of the first three products ignore any information regarding the behaviour when supplied with lower incoming pressures. For this reason a decision against these valves has been made. The process of ordering and testing these products would be too resource intensive for the scope of this project. Additionally there does not appear to be a standard conversion available, judging by the different responses that are documented for other low flow proportional valves [41, 42, 46]. Ultimately a decision for the Bürkert 274910 valve has been made, as the other remaining valve made by Parker was unable to be shipped within the desired time frame. Additionally, the 274910 appears to be the most flexible with a 1.2 l/min/bar flow. This allows any range of flow between 0-2 l/min with incoming pressures lower than 1.7 bar, including a 0.5 l/min at 0.7 bar.

### 3.3 Gas flow sensor

As with the previous subsection, the results following section 4.2 find a maximum steady state carbogen flow of 0.5 l/min. Therefore, all ranges of the sensors found in table 4 suffice. When comparing cost and accuracy there seem to be two competitors. The D6F-P0010A1 appears to be the low cost low accuracy winner. The AWM3300V is three times as accurate as the remaining sensors while being of similar cost. The budget allows the extra cost of the AWM3300V, therefore a choice for the extra accuracy has been made.

### 3.4 Feedback loop design

The design of the feedback loop consists of two proportional–integral–derivative (PID) controllers. PID controllers are error based feedback loops. The error is the difference between the setpoint the system aims to achieve and the calibrated value the sensor measures. A combination of the three elements (proportional, integral and derivative) determine how much the control adjusts for a given error.

A diagram of the double feedback loop design can be seen in figure 9. The inner (green) PID controller takes care of the carbogen flow. This allows the proportional valve to get adjusted to the feedback gained from the gas flow sensor that monitors the carbogen flow. Using the oxygen sensor, the outer (orange) feedback loop determines the setpoint of the inner (green) loop. Ultimately this means that the system can achieve the goal of adjusting the proportional valve such that a desired oxygen level in the perfusion solution is met.

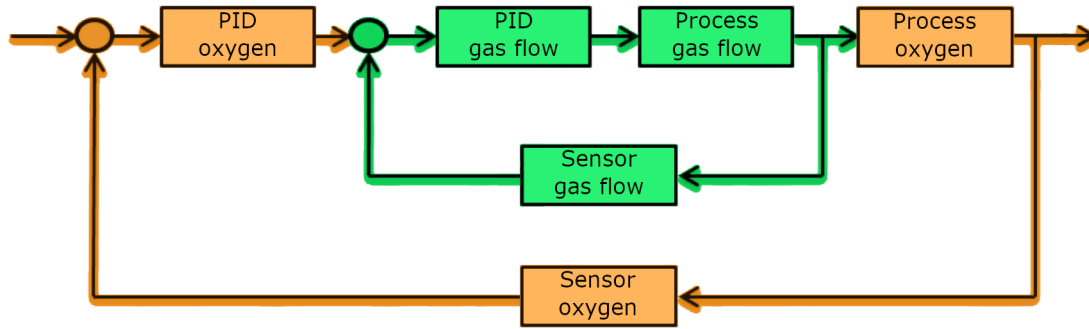


Figure 9: Diagram of the PID control, the gas flow PID (green) nested inside of the oxygen PID (orange).

The decision of using two loops instead of one larger feedback loop was made for multiple reasons. Firstly, it allows for the development to be done in smaller consecutive steps. Separating a task into smaller and thus less complex steps may prevent mistakes. Secondly, it enhances the ease of debugging, during the development but also after production. Enabling the ability to check whether smaller steps of an overall system are done successfully allows for more efficient trouble shooting. Lastly, it increases the flexibility of the system, as one could take out the inner (green) loop and use it in a different setup without much modifications.

## 4 Research design

### 4.1 Response time of the oxygen sensor

Two experiments have been performed in order to investigate whether the response time of the oxygen sensor fits within the requirements. The combination of these experiments will assist in the decision making concerning the oxygen sensor.

#### 4.1.1 Effect of flow rate

One could hypothesise that the flow of the perfusion solution may influence the time in which the sensor responds to a change in oxygen level. In order to find out whether this variable would influence the response time an experiment was set up. A diagram of the setup can be seen in figure 10:

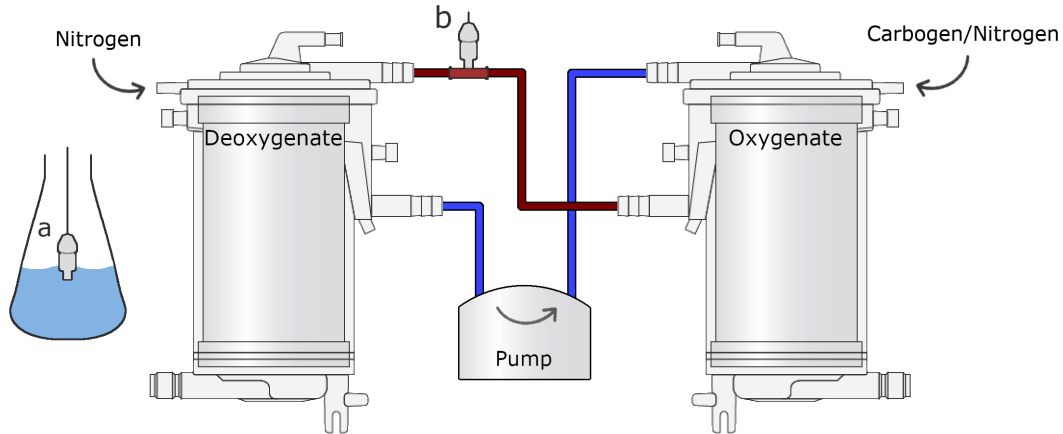


Figure 10: Schematic representation of the response time experiment setup.

By supplying the left oxygenator with nitrogen its goal is to remove the oxygen from the water by replacing it with nitrogen. By adjusting the mixture of carbogen and nitrogen supplied to the right oxygenator different oxygen levels in the water at point b can be achieved. Water was chosen over possible perfusion solutions, as no reason to do so seemed to outweigh the financial and ethical benefits of water. Once a desired stable oxygen level at point b was achieved, the sensor would move to point a. After a stable reading is achieved at point a, the sensor would be moved back to point b. The time the sensors takes to read the original reading at point b again will be considered the response time, within the margin of the documented accuracy. Important to note is that the gaseous supplies during this experiment is achieved by the use of the available rotameters.

To test whether the flow of the water has an influence two different groups have been created. One with a low flow, another with a high flow. If these groups have a statistically significant difference then the flow variable will have to be taken into account in the following response time experiment.

#### 4.1.2 Response time to different deltas

One of the characteristics of dissolved oxygen sensors is their relatively high response time. The response time of the sensor used during this project, the FTC-PSt3, is  $<40$  seconds, defined as 90% of the signal measured during a transition from an air saturated to an oxygen deprived solution [36]. However, from this information we cannot derive whether this response time is suitable for the project. This experiment has been created to find whether the maximum change of 325.8 hPa/min can be achieved by the sensor (see section 2.8 for more information).



Following the results found in section 5.1.1 can be concluded that the flow has an influence on the response time. The lower the flow, the lower the response time. Therefore this experiment will use the minimum flow specified in the documentation of the oxygenator, 150 ml/min [36].

The overall setup was identical to the one in section 4.1.1. However, during this experiment the groups were subjected to different oxygen deltas between point a and b. The flow of the water was kept at a constant for all the groups in this experiment.

## 4.2 Desired steady state of the gas mixture

To aid the decision making regarding the purchasing of the proportional valve and gas flow sensor combination an experiment was performed. This experiment aims to investigate the desired ratio in which the nitrogen and carbogen have to be presented to the oxygenator in order to achieve desired oxygen levels in the perfusion solution. In figure 11 a diagram of the setup can be found:

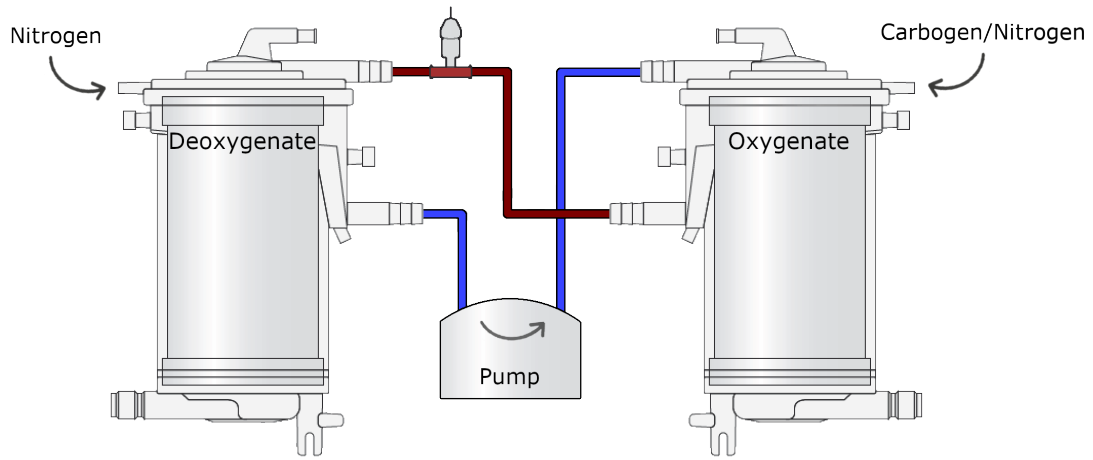


Figure 11: Schematic representation of the desired steady state setup.

As can be seen, the setup is similar to the previous experiments. The nitrogen removing the oxygen and the dynamic carbogen and nitrogen supply principles remain. However, a porcine blood based perfusion solution has replaced the water. Different carbogen and nitrogen ratios will be supplied to the right oxygenator and will be adjusted until an oxygen pressure of 133 hPa is measured.

The carbogen flow was measured using a oxygen calibrated rotameter, the nitrogen flow was measured using a nitrous oxide rotameter. Using the method explained in section 2.6 the following two rotameter conversions have been used:

Oxygen to carbogen:

$$K = \sqrt{\frac{1.429}{1.456}} = 0.991$$

Nitrous oxide to nitrogen:

$$K = \sqrt{\frac{1.834}{1.251}} = 1.211$$

### 4.3 Gas flow subsystem

The double feedback loop design discussed in the conceptual model (see section 3) includes the gas flow subsystem. This section includes two experiments that have been performed in order to complete this subsystem, such that it can later be incorporated into the full system.

#### 4.3.1 Sensor calibration

The gas flow sensor required calibration. Using a rotameter, that has been calibrated for pure oxygen, the actual carbogen flow was found using the method explained previously (see section 2.6). The corresponding sensor readout was saved. The result of this allows to convert the sensor readout to a measurement in ml/min.

The rotameter conversion calculation:

$$K = \sqrt{\frac{1.429}{1.456}} = 0.991$$

#### 4.3.2 PID tuning

The gas flow feedback loop requires to know how much it should adjust the proportional valve given an error. This error is the difference between the measured and the desired carbogen gas flow. To achieve this a set of step inputs will be administered to the system. These step inputs create a sudden change in how open the valve is. During this time the resulting flow will be measured.

Using this data the software called *Tune Wizard* (PAS Global, Houston Texas) will be used to create a corresponding mathematical model. This model is then used to derive the proportional, integral and derivative gain. Using these gains the system is informed how much it should change the openness of the valve given an error in gas flow. Figure 12 shows the corresponding feedback loop diagram:

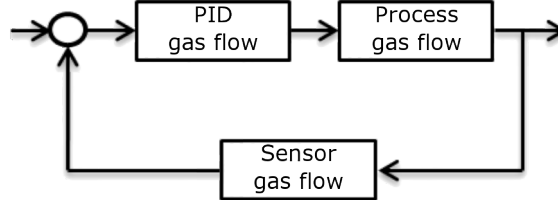


Figure 12: Diagram of the PID control which will be tuned in this experiment. Diagram identical to the inner (green) loop seen in figure 9.

### 4.4 Oxygen PID tuning

This experiment is the first experiment in which the full setup explained in section 3 and seen in figure 8 was deployed, thus including a porcine kidney. The only exclusion was the automation part of the outer feedback loop seen in figure 13, as the proportional, integral and derivative gains for this PID loop were unknown before this experiment.

Rather than directly dictating the openness of the valve the gas flow subsystem is dictated to create step inputs by changing its carbogen flow setpoint. Ultimately, this creates different oxygen levels in the perfusion solution that enters the kidney. As different oxygen levels entered the kidney, the oxygen levels leaving the kidney were also expected to differ. These resulting venous oxygen levels were saved, such that the required gains can now be calculated in similar fashion as explained in section 4.3.2.

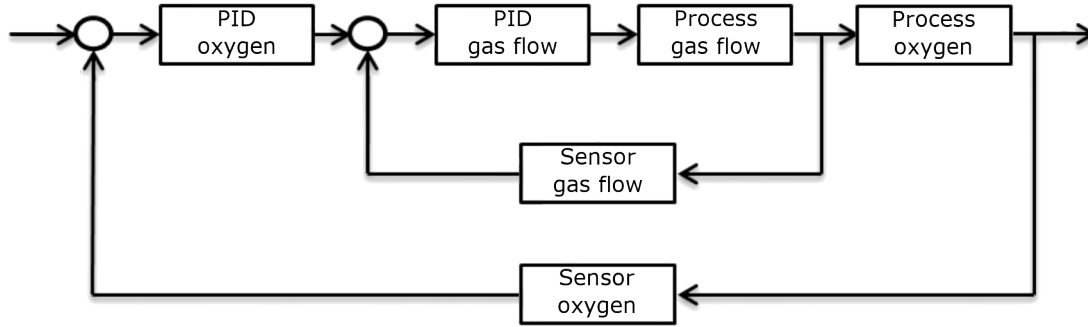


Figure 13: Diagram of the PID control. The outer loop has been tuned in this experiment. Diagram identical to the loop seen in figure 9, excluding the colors.

## 4.5 Validation

After the entire system was tuned it was ready to undergo a validation procedure. This procedure could involve just letting the system achieve its oxygen level setpoint and keep it there for the remainder of several hours. However, such an experiment would not stress test the system, as the change in metabolic rate would be expected change gradually. For a more drastic test a decision was made to let the system achieve its venous oxygen setpoint and then lower the temperature from the normothermic  $37^{\circ}\text{C}$  back to room temperature.

In order to achieve normothermic temperatures three pieces of equipment are typically used. A chamber to isolate the perfusion machine, a little heater to warm the air inside the chamber and a waterbath. This waterbath warms its water and pumps it into the heat exchanging part of the oxygenator. There the energy of the water is transferred to the perfusion solution. In order to decrease the temperature during this experiment the chamber was opened, the heater and waterbath turned off and ice was thrown in the waterbath.

The system of this project would have to adjust for the associated change in metabolic rate by responding with a different amount of supplied oxygen.

## 5 Results

### 5.1 Response time of the oxygen sensor

#### 5.1.1 Effect of flow rate

During the experiment that investigated the effect of the flow rate on the response time of the dissolved oxygen sensor the following results were created, see table 5:

Run	Group 150 ml/min response time (s)	Group 575 ml/min response time (s)
1	49	29
2	58	29
3	48	27
4	51	30
5	54	30
Mean	52	29

Table 5: Table with results of the effect of flow rate on the response time of the dissolved oxygen sensor. First group experienced a flow rate of 150 ml/min, the second group 575 ml/min.

From this table a histogram including the statistical significance has been created, see figure 14:

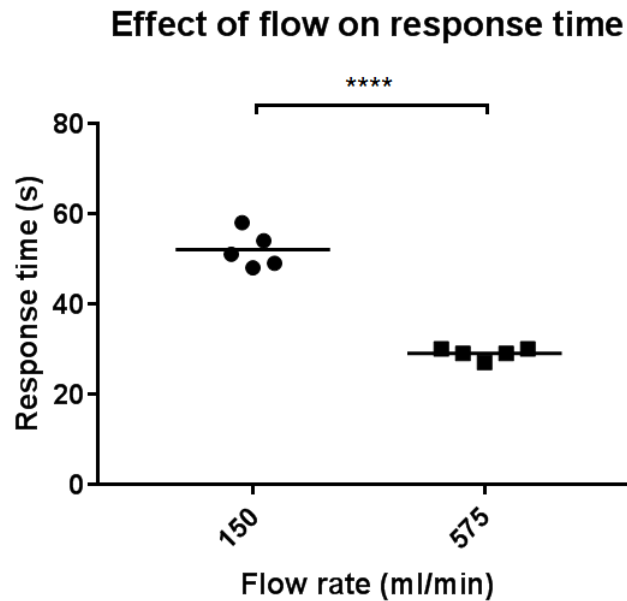


Figure 14: Histogram of the results of the effect of flow rate on the response time of the dissolved oxygen sensor. First group experienced a flow rate of 150 ml/min, the second group 575 ml/min. A statistical significant difference between the two groups was observed.

From the statistical significance between the two groups can be concluded that the flow rate does have an influence on the response time. A lower flow rate results in a lower response time. This information was used in the following experiment.

### 5.1.2 Response time to different deltas

Following the results of the previous experiment are the response times to different deltas. The results of the response time of the dissolved oxygen sensor of this experiment can be found in table 6:

Run	$\Delta 300$ hPa response time (s)	$\Delta 350$ hPa response time (s)	$\Delta 400$ hPa response time (s)	$\Delta 610$ hPa response time (s)
1	46	48	49	62
2	50	45	58	60
3	49	47	48	61
4	48	50	51	57
5	48	49	54	55
Avg.	48.2	47.8	52	59

Table 6: Table with results of the response times to different changes in oxygen level. The group with a 610  $\Delta$ hPa was added to investigate statistical difference.

From the table the following histogram was created. See figure 15:

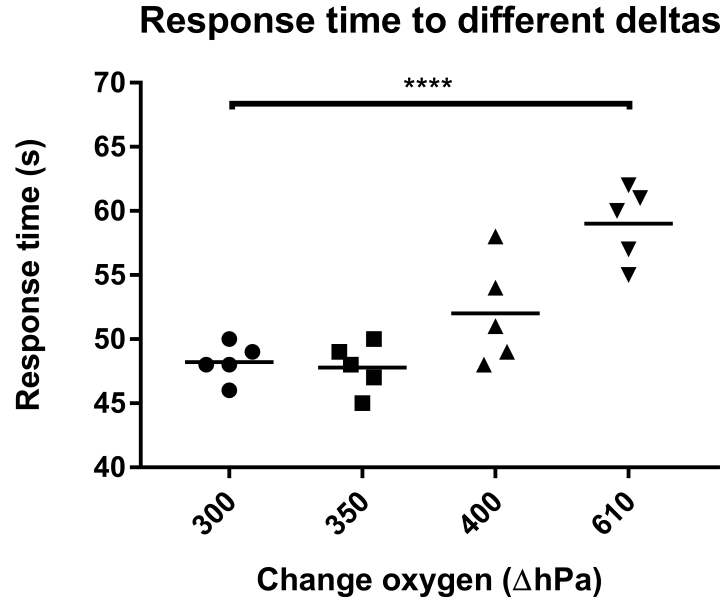


Figure 15: Graph.

All measurements taken stayed within the 60 seconds response time, excluding the group that experienced a 610  $\Delta$ hPa. The latter group having two measurements outside of the 60 seconds response time mark.

## 5.2 Desired steady state of the gas mixture

The results of the experiment that researched the ratio between nitrogen and carbogen supplied to the oxygenator, in order to achieve an oxygen level of 133 hPa, can be found in table 7:

Measured carbogen flow (l/min)	Adjusted carbogen flow (ml/min)	Measured N2 flow (l/min)	Adjusted N2 flow (ml/min)
0.17	168.4	0.5	525
0.25	247.7	0.65	682.5
0.48	475.5	1	1050
0.09	89.2	0.25	262.5
0.81	802.5	1.5	1575
0.34	336.8	0.75	787.5
0.66	653.9	1.25	1312.5

Table 7: Table with the results of the experiment that researched the ratio between nitrogen and carbogen supplied to the oxygenator in order to find a 133 hPa dissolved oxygen level.

The seemingly linear relation between the nitrogen and carbogen have been plotted in figure 16, alongside a linear fit:

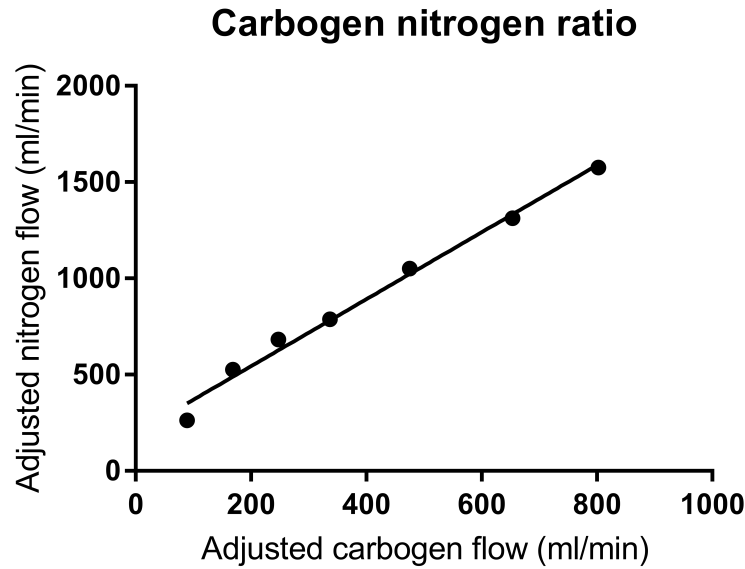


Figure 16: Graph of the ratio between nitrogen and carbogen in order to achieve an oxygen level of 133 hPa, alongside a linear fit.

These results guided the decision making regarding the proportional valve and the gas flow sensor (see section 3).

## 5.3 Gas flow subsystem

### 5.3.1 Sensor calibration

The results of the gas flow sensor calibration can be found in table 8:

Signal 1 (0-1023)	Signal 2 (0-1023)	Signal 3 (0-1023)	Average (0-1023)	Measured flow (ml/min)	Adjusted flow (ml/min)
202	204	206	204	0	0
395	393	394	394	100	99.1
539	546	541	542	200	198.2
661	658	661	660	300	297.2
751	748	751	750	400	396.3
806	816	814	812	500	495.3
860	854	863	859	600	594.4
921	930	921	924	700	693.5
953	944	950	949	800	792.5
989	994	990	991	900	891.6
1020	1012	1022	1018	1000	990.7

Table 8: Calibration results for the gas flow sensor.

Plotting this data shows a graph that does not appear to be linear, see figure 17:

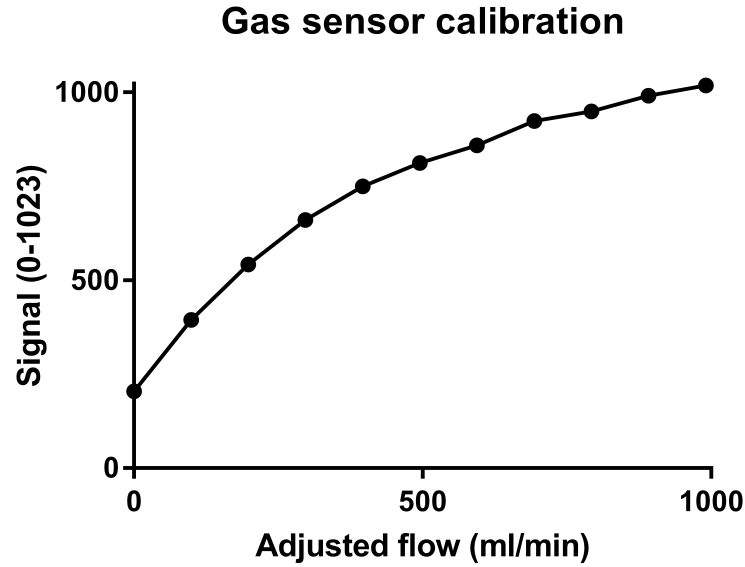


Figure 17: Graph.

A graph fit solution could provide the calibration equation. However, the resulting equation would be expensive in terms of processing power for the embedded system. Therefore the following consecutively ordered linear equations are used, expressed in C++ code:

```
// C++ implementation of the gas flow calibration

double CalibrationFunction(double analog) {
    if (analog < 205) return 0;
    else if (analog < 395) return 0.521413 * analog - 106.3682;
    else if (analog < 543) return 0.6693815 * analog - 164.6679;
    else if (analog < 661) return 0.8395632 * analog - 256.9064;
    else if (analog < 752) return 1.088664 * analog - 421.3131;
    else if (analog < 813) return 1.624073 * analog - 823.4051;
    else if (analog < 858) return 2.10784 * analog - 1216.223;
    else if (analog < 925) return 1.52413 * analog - 714.8171;
    else if (analog < 950) return 3.962739 * analog - 2968.091;
    else if (analog < 992) return 2.358773 * analog - 1445.928;
    else if (analog < 1024) return 3.669202 * analog - 2744.563;
}
```



### 5.3.2 PID tuning

The PID tuning data regarding the gas flow subsystem can be seen in figure 18. This plot includes the input (green), which is the valve openness and the resulting gas flow (blue). After the experiment the data was fed into the PID tuning software.

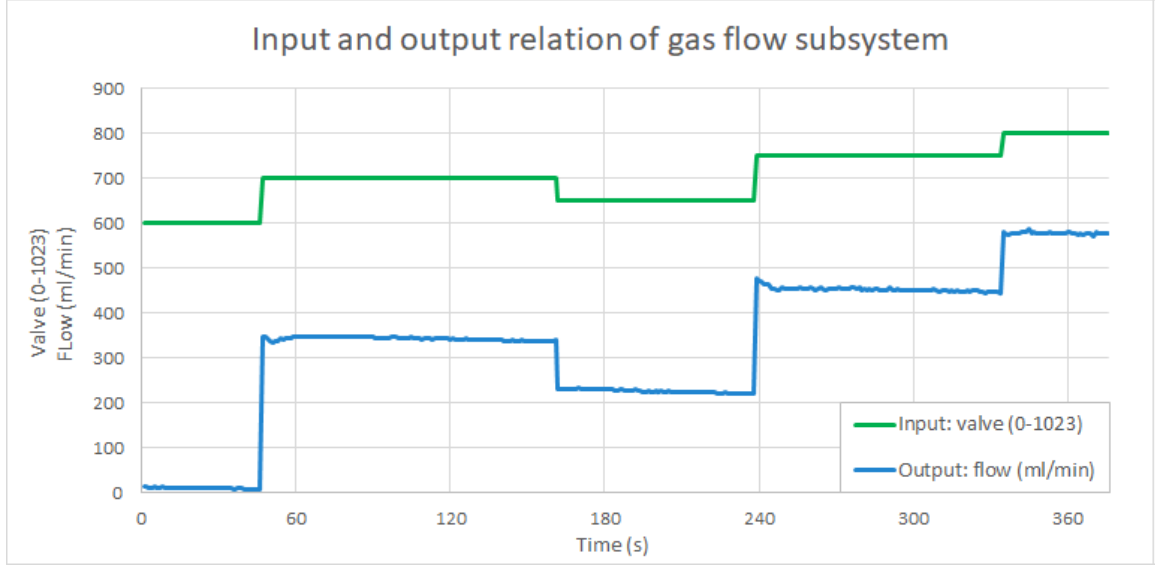


Figure 18: Plots of the input and resulting output of the gas flow subsystem during a series of step inputs.

The purpose of the model that is created is to gain a mathematical understanding of the relationship between the previously observed input and output. Given the same input as the actual system, the mathematical model responds as seen in figure 19:

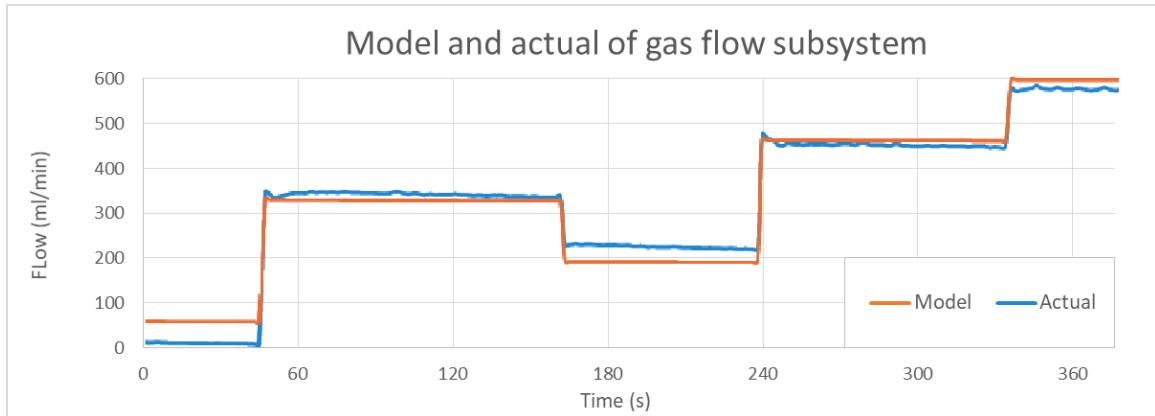


Figure 19: Plots of the response of the mathematical model and the actual response given the same input, for the gas flow subsystem.

However, the purpose of the model should not be confused. The model will not be used calculate the desired openness of the valve for a given flow. Instead the model is used to calculated the three gains which can be found in table 9:

Proportional gain	Integral gain	Derivative gain
0.090	0.18	0

Table 9: Table of proportional, integral and derivative gain for the gas flow subsystem.

## 5.4 Oxygen PID tuning

In similar fashion as in the previous experiment, the oxygen feedback loop was submitted to a series of step inputs. In figure 20 the input (green) and the resulting output (blue) can be found:

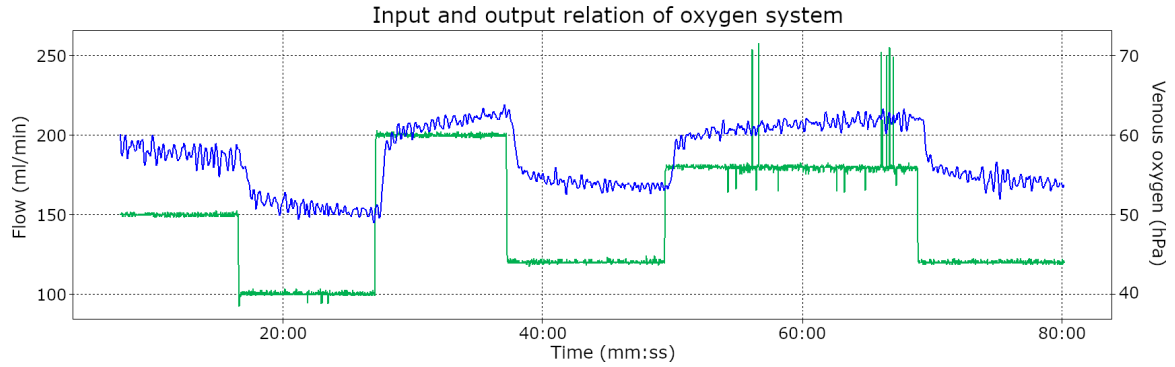


Figure 20: Plots of the input and resulting output of the full system during a series of step inputs. Input in carbogen flow (ml/min) depicted in green, output in venous oxygen level (hPa) depicted in blue.

Again in similar fashion as the previous experiment a mathematical model was created. The response of the mathematical model and the actual response are plotted in figure 21:

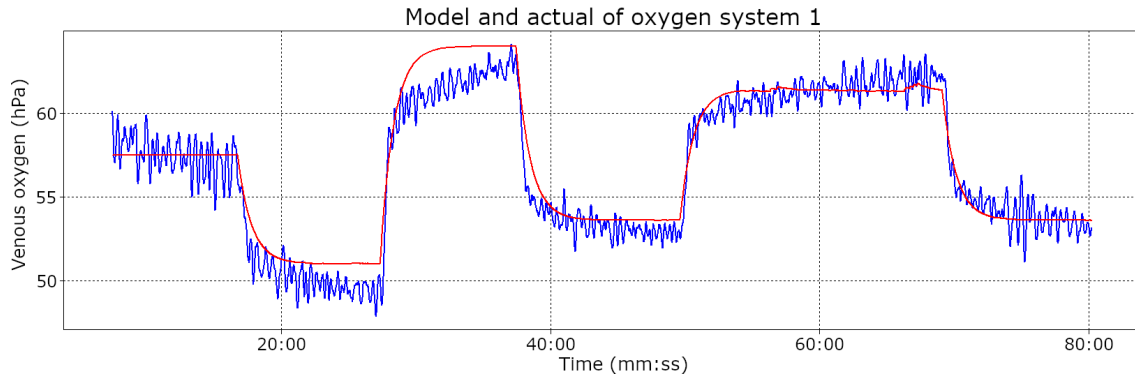


Figure 21: Plots of the response of the mathematical model and the actual response given the same input, for the full system. Mathematical model depicted in red, actual model in blue.

The process above was repeated, the model and the actual response can be seen in figure 22. However, this second set of data includes one small difference. The kidney during the second run was the same kidney after a pilot of the validation experiment. This was done for financial reasons as well as time efficiency. During this pilot the kidney endured multiple ischemic periods due to technical difficulties. Consequently the expected metabolic rate is lower than what it would have been at the beginning of the pilot.

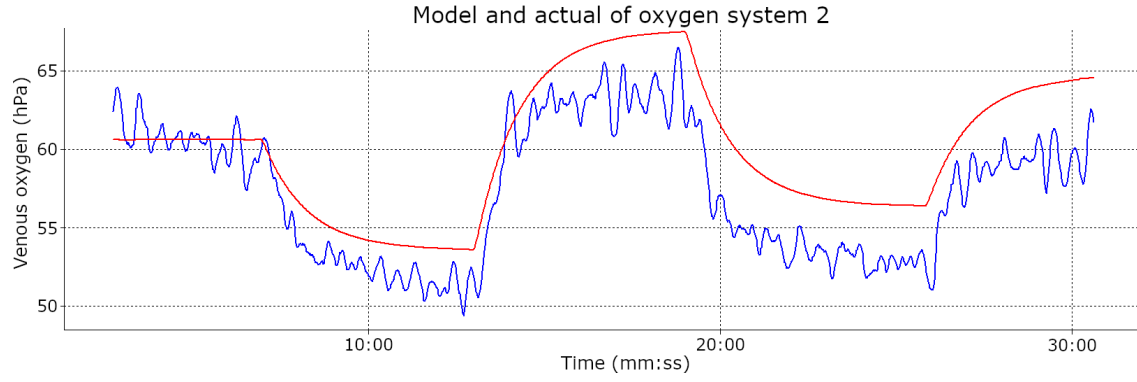


Figure 22: Second set of plots of the response of the mathematical model and the actual reponse given the same input, for the full system. Mathematical model depicted in red, actual model in blue. Kidney endured multiple ischemic periods and data of the last step impulse was lost due to technical difficulties.

The resulting gains of the above models can be found in table 10.

	Proportional gain	Integral gain	Derivative gain
Kidney 1	5.7	0.89	0.12
Kidney 2	5.8	1.2	0.088

Table 10: Table of gains from two different kidneys subjected to identical step inputs.

## 5.5 Validation

The following graphs are all from the same validation experiment. All of the data was measured simultaneously, meaning that all horizontal axes are identical for the the graphs 23, 24, 25 and 26:

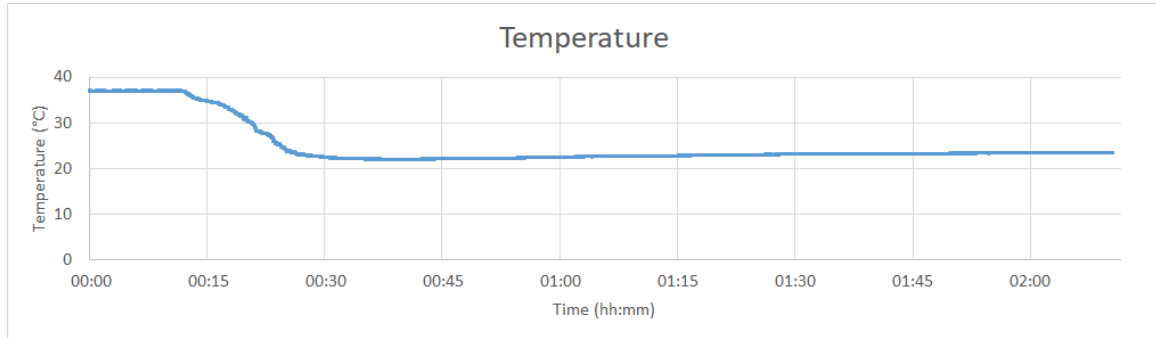


Figure 23: Graph with temperature data of the validation experiment.

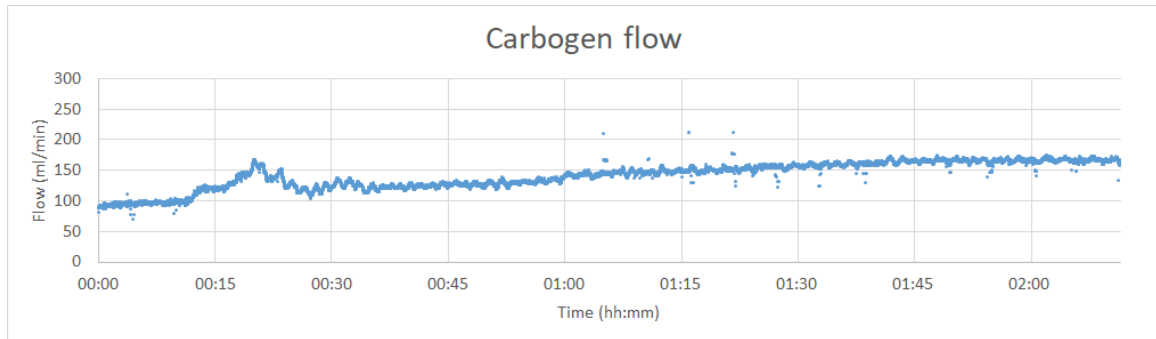


Figure 24: Graph with carbogen flow data of the validation experiment.

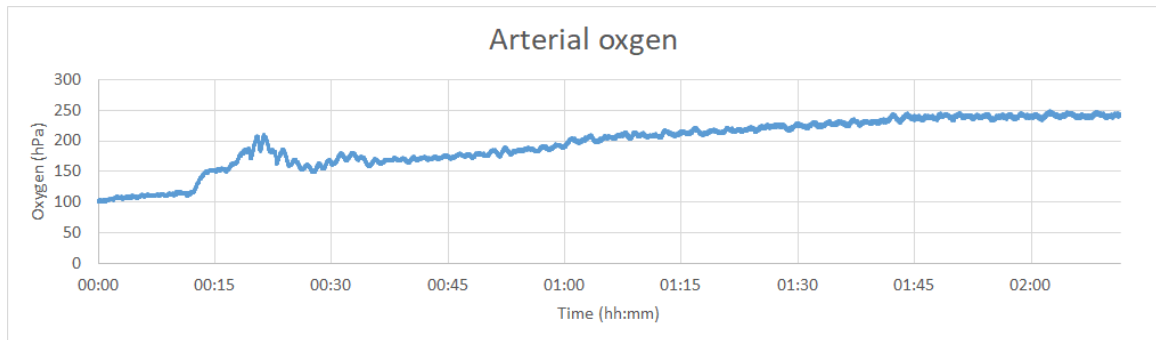
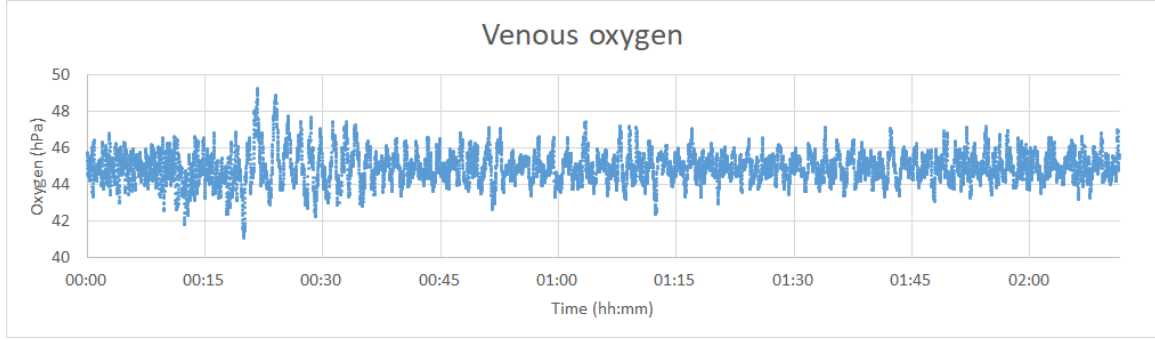


Figure 25: Graph with arterial oxygen pressure data of the validation experiment.



*Figure 26: Graph with venous oxygen pressure data of the validation experiment.*

The temperature, measured in the perfusion solution, was successfully decreased to room temperature in approximately 15 minutes. During this time the system responded with increasing the carbogen flow, consequently the arterial oxygen level followed. This was done in order to attempt to achieve the goal of keeping the venous oxygen level at 45 hPa. The lowest measured oxygen level was 41.08 hPa, the highest 49.16 hPa. Meaning that the system was able to stay within a  $\pm 4.16$  hPa range of its setpoint.

Figure 27 and 28 were taken during the validation experiment:

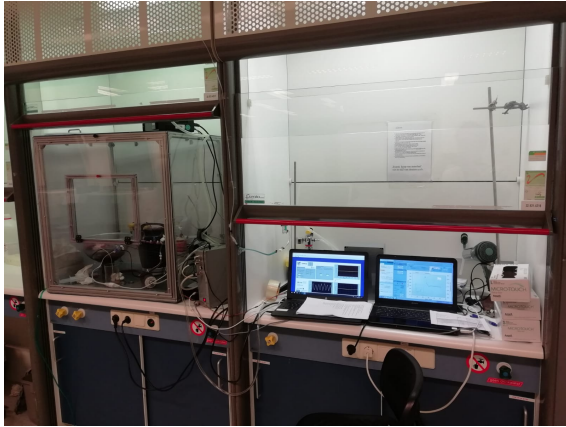


*Figure 27: Photo of the entire setup during the validation experiment.*

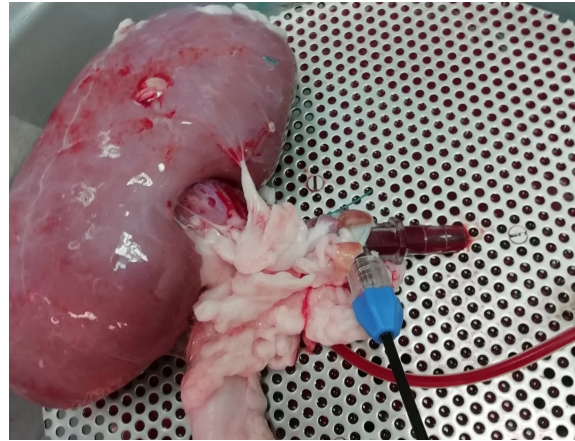


*Figure 28: Photo of the kidney during the validation experiment.*

## 6 Conclusion

In conclusion this project has achieved to add to the current perfusion machine a system that can dynamically control the oxygen level and may adjust to the metabolic rate of the kidney. During the stress test in the validation process the system was able to stay within  $\pm 4.16$  hPa of its 45 hPa setpoint (n=1).

From literature and within the scope of the project the dissolved oxygen sensors appeared to be the best fit for oxygen monitoring. The experiments conducted showed that the dissolved oxygen sensor PreSens FTC-PSt3 meets the response time requirement of at least 325.8 hPa/min. This sensor was used in the prototype.

Furthermore, the concept of combining carbogen and nitrogen to the supply of the oxygenator was shown to successfully influence the oxygen levels. The proportional valve Bürkert 274910 and gas flow sensor Honeywell AWM3300V have been able to complete the realisation of this concept.

The concept of measuring and adjusting over the venous oxygen levels appears to adjust for the change in metabolic rate of the kidney. However, more research regarding the success of the implementation is required.

## 7 Discussion

To be added.

## 8 List of definitions

Anemia - A condition in which there is a deficiency of red cells or of hemoglobin in the blood, resulting in pallor and weariness.

DNA - Deoxyribonucleic acid.

Graft - A piece of living tissue that is transplanted surgically.

HMP - Hypothermic machine perfusion.

Hyperoxia - An excess in the amount of oxygen reaching the tissue.

Hypothermia - The condition of having an abnormally low body temperature.

IRI - ischemia-reperfusion injury.

Ischemia - An inadequate blood and oxygen supply to an organ or part of the body, especially the heart muscles.

MP - Machine perfusion.

NMP - Normothermic machine perfusion.

Normothermia - Normal body temperature; the condition of having a normal body temperature.

ODC - Oxygen dissociation curve.

Perfusion - The passage of blood, a blood substitute, or other fluid through the blood vessels or other natural channels in an organ or tissue.

Supraphysiological - Higher in value than is normal in an animal or plant.

RAM - Random access memory.

Respiratory quotient - The ratio of the volume of carbon dioxide evolved to that of oxygen consumed by an organism, tissue, or cell in a given time.

RNA - Ribonucleic acid.

ROS - Reactive oxygen species.

RQ - Respiratory quotient.

UMCG - University Medical Center Groningen.

## 9 References

- [1] Patrizia Burra et al. “EASL clinical practice guidelines: liver transplantation”. In: *Journal of hepatology* 64.2 (2016), pp. 433–485.
- [2] Anne-Hélène Querard et al. “Comparison of survival outcomes between Expanded Criteria Donor and Standard Criteria Donor kidney transplant recipients: a systematic review and meta-analysis”. In: *Transplant International* 29.4 (2016), pp. 403–415.
- [3] H Groen et al. “Cost-effectiveness of hypothermic machine preservation versus static cold storage in renal transplantation”. In: *American Journal of Transplantation* 12.7 (2012), pp. 1824–1830.
- [4] J Moritz Kathz et al. “Ex vivo machine perfusion for renal graft preservation”. In: *Transplantation Reviews* 32.1 (2018), pp. 1–9.
- [5] Panxin Peng et al. “Hypothermic Machine Perfusion Versus Static Cold Storage in Deceased Donor Kidney Transplantation: A Systematic Review and Meta-Analysis of Randomized Controlled Trials”. In: *Artificial organs* (2018).
- [6] Jens Brockmann et al. “Normothermic perfusion: a new paradigm for organ preservation”. In: *Annals of surgery* 250.1 (2009), pp. 1–6.
- [7] Constantino Fondevila et al. “Superior preservation of DCD livers with continuous normothermic perfusion”. In: *Annals of surgery* 254.6 (2011), pp. 1000–1007.
- [8] Sarah A Hosgood and Michael L Nicholson. “Normothermic kidney preservation”. In: *Current opinion in organ transplantation* 16.2 (2011), pp. 169–173.
- [9] Nicholas Gilbo and Diethard Monbaliu. “Temperature and oxygenation during organ preservation: friends or foes?” In: *Current opinion in organ transplantation* 22.3 (2017), pp. 290–299.
- [10] Christopher JE Watson et al. “Normothermic Perfusion in the Assessment and Preservation of Declined Livers Before Transplantation: Hyperoxia and Vasoplegia—Important Lessons From the First 12 Cases”. In: *Transplantation* 101.5 (2017), p. 1084.
- [11] Ministerie van Natuur en Voedselkwaliteit Landbouw. *Dierproeven*. visited on 2019-04-26. Mar. 2017. URL: <https://www.ncadierproevenbeleid.nl/dierproeven-en-3V-methoden/d/dierproeven>.
- [12] Benjamin Dekel et al. “Human and porcine early kidney precursors as a new source for transplantation”. In: *Nature medicine* 9.1 (2003), p. 53.
- [13] Cyril Moers et al. “Machine perfusion or cold storage in deceased-donor kidney transplantation”. In: *New England Journal of Medicine* 360.1 (2009), pp. 7–19.
- [14] *Hilite 800 LT Serie Hilite 100 Serie. Instructions for use*. Medos Medizintechnik AG. Stolberg Germany, Aug. 2015.
- [15] P. W. Atkins. *Chemical Principles*. W.H. Freeman & Company, 2013. ISBN: 1464120676.
- [16] Julie-Ann Collins et al. “Relating oxygen partial pressure, saturation and content: the haemoglobin–oxygen dissociation curve”. In: *Breathe* 11.3 (2015), pp. 194–201.
- [17] Ranjan K Dash, Ben Korman, and James B Bassingthwaighe. “Simple accurate mathematical models of blood HbO<sub>2</sub> and HbCO<sub>2</sub> dissociation curves at varied physiological conditions: evaluation and comparison with other models”. In: *European journal of applied physiology* 116.1 (2016), pp. 97–113.
- [18] C Bohr, K Hasselbalch, and A Krogh. “Concerning a biologically important relationship—the influence of the carbon dioxide content of blood on its oxygen binding”. In: *Skand. Arch. Physiol* 16 (1904), pp. 402–412.
- [19] Donald Voet, Judith G. Voet, and Charlotte W. Pratt. *Fundamentals of Biochemistry: Life at the Molecular Level*. Wiley, 2008. ISBN: 0470129301.



- [20] N Naeraa et al. “pH and molecular CO<sub>2</sub> components of the Bohr effect in human blood”. In: *Scandinavian journal of clinical and laboratory investigation* 18.1 (1966), pp. 96–102.
- [21] Neil A. Campbell. *Biology: A Global Approach*. Pearson Education Limited, 2014. ISBN: 1292008652.
- [22] Amy Uber et al. “Preliminary observations in systemic oxygen consumption during targeted temperature management after cardiac arrest”. In: *Resuscitation* 127 (2018), pp. 89–94.
- [23] Robert Brooker. *Genetics: Analysis and Principles*. McGraw-Hill Science/Engineering/Math, 2011. ISBN: 0073525286.
- [24] Jeremy PT Ward. “Oxygen sensors in context”. In: *Biochimica et Biophysica Acta (BBA)-Bioenergetics* 1777.1 (2008), pp. 1–14.
- [25] Kimberly J Dunham-Snary et al. “A mitochondrial redox oxygen sensor in the pulmonary vasculature and ductus arteriosus”. In: *Pflügers Archiv-European Journal of Physiology* 468.1 (2016), pp. 43–58.
- [26] Iris Schmidt. “Universitair Medisch Centrum Groningen (UMCG)-designed oxygenator as a low-budget oxygenator for kidney perfusion - a prospective study”. unpublished. 2016.
- [27] HH Dijstelbergen. “Rotameter dynamics”. In: *Chemical Engineering Science* 19.11 (1964), pp. 853–865.
- [28] G Rollmann. “Calculation of correction factors for variable area flow meters at deviating working conditions”. In: *Cerca con Google* ().
- [29] J Moritz Kathes et al. “Ex vivo machine perfusion for renal graft preservation”. In: *Transplantation Reviews* 32.1 (2018), pp. 1–9.
- [30] Przemyslaw David Kosinski. “MR-Based Mapping of Cerebral Hemodynamics in Children with Sick Cell Disease”. PhD thesis. 2016.
- [31] John W Severinghaus and Poul B Astrup. “History of blood gas analysis. VI. Oximetry”. In: *Journal of clinical monitoring* 2.4 (1986), pp. 270–288.
- [32] James E Sinex. “Pulse oximetry: principles and limitations”. In: *The American journal of emergency medicine* 17.1 (1999), pp. 59–66.
- [33] Stephen Bell and Frank Dunand. “A comparison of amperometric and optical dissolved oxygen sensors in power and industrial water applications at low oxygen levels”. In: *Power Plant Chemistry* 12.5 (2010), pp. 296–303.
- [34] Stephen Bell et al. “Optical dissolved oxygen measurement in power plants—A comparison of amperometric and optical dissolved oxygen sensors for applications at low oxygen levels”. In: *VGB PowerTech* 92.9 (2012), p. 119.
- [35] *NeoFox Phase Fluorometer Installation and Operation Manual*. Ocean Optics Inc. Dunedin USA, 2010.
- [36] *Optical Oxygen Sensors & Meters*. PreSens Precision Sensing. Regensburg Germany, Jan. 2018.
- [37] *Flow-Through Cells with Optical Oxygen and Temperature Sensor*. PyroScience GmbH. Aachen Germany.
- [38] *Miniature proportional volume flow regulator PVK*. AirCom Pneumatic GmbH. Ratingen Germany, 2011.
- [39] *Miniature-proportional-flow-valve PV202*. AirCom Pneumatic GmbH. Ratingen Germany, 2011.
- [40] *2/2 Brass & Stainless*. Baccara. Geva Israel, 2010.
- [41] *Direct-acting 2-way standard solenoid control valve*. Bürkert Contromatic BV. Breda the Netherlands, May 2018.
- [42] *VSO Low Flow*. Parker Hannifin Corp. Cleveland USA, May 2017.
- [43] *Airflow Sensors AWM3000 Series*. Honeywell Inc. Freeport USA.
- [44] *D6F-P*. Omron. Schaumburg Germany.

- [45] *D6F-01A1 -02A1*. Omron. Schaumburg Germany.
- [46] *Lone Wolf. Normally Open Miniature Proportional Valve*. Parker Hannifin Corp. Cleveland USA, Mar. 2019.

## 10 Appendix

### A Sniffing the random access memory for data acquisition

Rather than the actual EOM-O2-FOM mentioned in table 2, the lab owns the Fibox 4. These products are both meant as interfacing modules for the PreSens dissolved oxygen sensor. Unfortunately, the Fibox 4 is meant to exclusively communicate with a standard computer, in contrast to the EOM-O2-FOM. Additionally, the software that comes with the Fibox does not have functionality that allows real-time communication with external hardware. Therefore another solution to this challenge has to be found, as the project does not have the budget to solve this by purchasing the required hardware.

Software that is installed on a computer is saved on the hard drive, or more recently on a solid state drive. Which function identical within the scope of this project. Whenever the software is loaded it gets stored onto the random access memory (RAM). The reason for this is that the RAM is much quicker, thus improving the responsiveness of the system. Unfortunately RAM is more expensive and loses the data that is stored in it once it is shut down. In the context of the PreSens software, the measurement lives somewhere in the RAM once the user has opened the software and has started measuring. Which means it is possible to read out the RAM and obtain the current measurement. However, this is more complex then it might appear.

Whenever the user opens software the operation system, Windows in this case, is asked to assign a certain amount of RAM to the software. Which addresses of the RAM get assigned to the software is dynamic, as different portions of the RAM might be open at the instance of opening the software. Fortunately, with the right amount of administrator privileges a process can request the addresses assigned to specific software.

However the address of the measurement within the assigned addresses is also dynamic. A solution to this challenge is to find a certain pathway from a static address that will lead towards the dynamic measurement address. Software called Cheat Engine allows to search for this pathway. This can be done by opening the PreSens software and doing one measurement. Then load Cheat Engine, attach it to the Presens software and start searching for the mesaured value. Now, in the PreSens software a new measurement is taken. From all of the previously found addresses in Cheat Engine search for the new measurement. Repeat this process until one address remains.

Now that the correct address is found we could use this to read the hPa value with external software. However, would the PreSens software be closed and reopened the address the current measurement lives is on different address, rendering the old address useless for the intended purposes. In order to solve this Cheat Engine can be tasked to find all address that access the address of interest. Not only can it search for the addresses that access the found address, it can do this for the addresses that access those new addresses as well. This can easily repeat itself multiple levels deep. This list of addresses and corresponding pointers to the deeper level addresses is saved. Now the Presens software should be closed and reopened. Once the entire process of finding the value of interest and creating the list of addresses and pointers is completed two lists have been obtained.

These two lists, after adjusting for the offsets of the dynamically assigned starting address by the operating system, are essentially the same. The only difference between the two lists are the differences created by the dynamicity of the software. By comparing the two lists and removing all of the previously mentioned differences one lists remains. This new list starts with a static addresses and pointers that move through multiple levels to eventually all lead towards the address of the measurement.

By using one of the found pathways to the measurement newly written software should be able to consistently find the measurement value in the RAM. First the new software has to obtain the

address assigned by the operating system and then use the pathway to find the value of interest. Additionally this software can then send the value to external hardware.

*Cheat Engine software source: <https://www.cheatengine.org/>*

## **B To be added**

Remainder of appendix to be added.